1 **Title**

2 **The genetic relevance of human iPSC-derived microglia to Alzheimer's disease and**

3 **major neuropsychiatric disorders**

4

5 Authors:

6 Robert R. Butler III[1,2#], Alena Kozlova[1,2#], Hanwen Zhang[1], Siwei Zhang[1,2], Michael Streit[1], Alan

7 R. Sanders[1,2], Krzysztof Laudanski[3,4], Zhiping P. Pang[5], Pablo V. Gejman[1,2], Jubao Duan[1,2*]

8

9 [1] Center for Psychiatric Genetics, NorthShore University HealthSystem, Evanston, IL 60201,

10 USA

11 [2] Department of Psychiatry of Behavioral Neuroscience, The University of Chicago, IL 60611,

12 USA

13 [3]Department of Anesthesiology and Critical Care, The University of Pennsylvania, Philadelphia,

14 PA 19104

15 [4]Institute for Translation Medicine and Therapeutics, The University of Pennsylvania, PA 19104

16 [5] Department of Neuroscience and Cell Biology and Child Health Institute of New Jersey,

17 Rutgers University, New Brunswick, NJ 08901, USA

18

19 [#] Equal contribution

20 * Correspondence: jduan@uchicago.edu

21

22

Abstract

Microglia are the primary innate immune cell type in the brain that have been implicated in the pathogenesis of several neurodegenerative and neuropsychiatric disorders, most notably Alzheimer's disease (AD) and Schizophrenia (SCZ). Microglia generated from human-induced pluripotent stem cells (hiPSCs) represent a promising *in vitro* cellular model for studying the neuroimmune interactions involved in these disorders. Among several methods of generating hiPSC-derived microglia (iMG)—varying in duration and resultant purity—a recent protocol by Brownjohn et al. is particularly simple and efficient. However, the replicability of this method, transcriptomic similarity of these iMG to primary adult microglia, and their genetic relevance to disease (*i.e,* enrichment of disease risk loci in genes preferentially expressed in these cells) remains unclear. Using two hiPSC lines, we demonstrated that Brownjohn's protocol can rapidly generate iMG that morphologically and functionally resembled microglia. The iMG cells we generated were found to be transcriptionally similar to previously reported iMG, as well as fetal and adult microglia. Furthermore, by using cell type-specific gene expression to partition disease heritability, we showed that iMG cells are genetically relevant to AD but found no significant enrichments of risk loci of Parkinson's disease, schizophrenia, major depressive disorder, bipolar disorder, autism spectrum disorder, or body mass index. Across a range of neuronal and immune cell types we found only iMG, primary microglia, and microglia-like cell types exhibited a significant enrichment for AD heritability. Our results thus support the use of iMG as a human cellular model for understanding AD biology and underlying genetic factors, as well as for developing and efficiently screening new therapeutics.

44

Introduction

Alzheimer's disease (AD) is an age-related neurodegenerative disease that is characterized by a cognitive decline, with histological hallmarks including the deposition of amyloid-beta (Aβ) plaques, the formation of neurofibrillary tangles, and neuroinflammation [1]. Genome-wide association studies (GWAS) on AD have identified more than 20 risk loci [2-5]. Putative AD-relevant genes near GWAS loci are highly expressed in immune-related tissues and cell types, in particular microglia [6,7]. Furthermore, recent single-cell RNA-seq profiling of an AD mouse model defined subtypes of microglia associated with different disease stages (i.e., homeostatic microglia, stage-1 trem2-independent disease associated microglia [DAM], and stage-2 trem2-dependent DAM) [8]. Given the limited overlap of transcriptomic profiles between humans and mice [9], studying AD genetic risk factors in human microglia cell models is important to understanding AD pathogenesis.

Microglia are the primary innate immune cells in the brain. Studying human microglia is understandably challenging due to the scarcity of living human brain tissue for research, or cadaver tissue artifacts. Generating *in vitro* human microglia from a renewable resource such as human-induced pluripotent stem cells (hiPSCs) provides an important alternative approach. Microglia originate from yolk sac macrophage progenitors during primitive hematopoiesis [10,11]. These primitive macrophages then migrate into the developing brain, become microglial progenitors, and finally mature microglia. They then function as immune cells, facilitate brain development, and modulate synaptic activity [12,13]. To mimic this unique developmental process, different methods have been recently developed to generate induced microglia (iMG) from hiPSCs [14-19]. These protocols differ in the use of different specific growth factors, co-culturing with other types of neuronal cells, starting from embryoid bodies (EBs) or monolayer cell culture, purity of the derived iMG, and the length of the differentiating time. Most recently, Brownjohn et al. [19] developed a simple method that generates functional iMG in large

71   numbers with near 100% purity within 20-30 days. It starts from EB-released primitive

72   macrophage precursors (PMPs) [19]. Because the EB-based approach historically lacks

73   reproducibility, the replicability of this protocol remains to be independently tested. Moreover, it

74   has not been demonstrated whether the resultant iMG cells are AD-relevant beyond their

75   molecular and transcriptomic resemblance to primary microglial cells, an essential component

76   for using iMG cells as a valid *in vitro* cellular model for understanding AD biology. This is valid

77   point since some microglia emerge from primitive EB precursors, but that knowledge is still

78   evolving. Finally, although complement C4 (C4A) has been implicated in schizophrenia (SCZ)

79   GWAS as a strong genetic risk factor and mechanistically linked to microglia-mediated

80   abnormal synapse pruning [20,21], it remains unknown whether iMG cells are a genetically

81   relevant cell type for SCZ.

82

83   Here, we first replicated the results reported by Brownjohn et al. [19], and found that the

84   transcriptomic profiles of our iMG were similar to that of previously reported iMG [15,19], as well

85   as fetal and adult microglia. By partitioning disease heritability of GWAS risk loci proximal to

86   genes specific to each cell type, we also demonstrated that iMG were a significantly enriched

87   cell type for AD risk—as were primary adult and fetal microglia—indicating the relevance of iMG

88   to AD. We compared this to enrichments for disease risk loci of Parkinson's disease (PD) and 4

89   other major psychiatric disorders—SCZ, major depressive disorder (MDD), bipolar disorder

90   (BIP), and autism spectrum disorder (ASD). Our results provide key support for using hiPSC-

91   derived iMG as a human cellular model to study the molecular/cellular mechanisms and genetic

92   risk factors of AD.

93

94   **Results**

95

96   **Replicability of Brownjohn's protocol [19] to generate iMG**

97   We selected two hiPSC lines (CD11 and CD21) well-characterized for pluripotency and absence

98   of cryptic chromosomal abnormalities (Fig. 1a, Supplementary Fig. 1a, b). As expected, EBs

99   were formed within 4 days after initiation of hiPSC differentiation, and PMPs were continuously

100   produced in suspension beyond 5 days (Fig. 1b). We found that a sufficient amount of PMPs

101   were released between days 14 and 32, with the greatest numbers of PMPs being produced

102   between days 14 and 19. The CD11 iMG were highly pure, with multiple cultures originating

103   from the different plated fractions of PMPs, extending 30 days from the earliest iMG

104   identification at day 24 (Fig. 1a). However, for the CD21 line, batches beyond the first collection

105   of PMPs gave rise to impure iMG cultures, with non-iMG cells increasing in concentration (Fig.

106   1b). The CD21-3 heterogeneous culture, generated from PMPs collected at day 23 harbored

107   50% non-iMG cells, and CD21-4 collected at day 39 were 100% non-iMG. These non-iMG cells

108   morphologically looked like fibroblasts, which was later confirmed as fibroblast-like by

109   transcriptomic analysis.

110

111   Regardless, we were able to successfully produce PMPs and iMG for both lines within the

112   expected time frame, as characterized by immunofluorescence (IF) staining of

113   macrophage/microglia -specific markers TREM2, CD45, and PU1 (Fig. 1c, d). Samples with

114   pure iMG by IF staining were further tested by qPCR for microglia-specific markers (Fig. 1e,

115   Supplementary Table 1). The iMG showed high-level expression of AD-associated genes,

116   TREM2 and APOE (Fig. 1e). Thus, we were able to confirm the overall transferability of the

117   Brownjohn's iMG protocol [19], producing preliminarily identified iMG. However, careful

118   monitoring for non-iMG cell encroachment is needed, because in some occasions fibroblast-like

119   cells may be observed in iMG culture (similar observation has also been observed in by the

120   authors of the original protocol [19]; personal correspondence).

121

122   **Functional validation of hiPSC-derived iMG**

123   We next examined whether the hiPSC-derived iMG were functionally similar to microglia (MGL).

124   One of the essential function of microglia is to phagocytose exogenous pathogens and cellular

125   debris [22]. Using pH-dependent fluorescence imaging we showed that iMG effectively

126   phagocytosed pHrodo-*E. coli*, and that phagocytosis continued over time. Thirty minutes after

127   adding pHrodo-*E. coli* to iMG, we detected fluorescence signal inside the cells that increased

128   rapidly through 150 minutes (Fig. 2a-c). This process is sensitive to cytochalasin D, an inhibitor

129   of actin polymerization, and when added to the culture prior to the pHrodo-*E.coli*, iMG cells lost

130   the ability to phagocytose bioparticles (Fig. 2d). Thus, our iMG cells engage in pathogen-

131   responsive phagocytic behavior that is a hallmark of MGL.

132

133   **Transcriptomic similarity of iMG and fetal/adult microglia (MGL)**

134   To examine how our iMG cells compare to previously reported iMG cells, fetal MGL (fMGL), and

135   adult MGL (aMGL), we first performed a principal component analysis (PCA) of transcriptomic

136   profiles from these and other non-microglial cells (Fig. 3a, Supplementary Table 2). The two

137   hiPSC lines used to generate our iMG and neural progenitor cells (NPCs) were clustered

138   together with other hiPSC lines that were previously used [15], suggesting a comparable quality

139   of source hiPSC lines between our current study and previous reports. Our high quality iMG

140   samples (CD11_1-6, CD21_1) were clustered together with previously reported iMG as well as

141   cultured fMGL and aMGL [15,19]. PMPs from our current study (CD11_7 and CD21_5) and

142   from previous reports were interspersed with iMG and fetal/adult MGL samples. Overall, PMPs,

143   iMG, and MGL samples were well separated from other cell types; the next closest cell type in

144   the first principal component, monocytes (MC), being effectively separated in the second

145   component (Fig. 3a). These observations were further corroborated by pairwise Poisson

146   distance, with the hierarchical heatmap clustering of gene expression showing a similar

147   grouping of samples (Fig. 3b).

148

149 Interestingly, our transcriptomic analyses showed that the observed "mixed" iMG samples,

150 CD21_3 and CD21_4, with heavy and almost total fibroblast-like cell overgrowth, clustered

151 together with fibroblast cells (Fib), while the sample with a less concentrated fibroblast-like

152 population (CD21_2) was located in between the fibroblasts and iMG (Fig.3a). The pairwise

153 clustering heatmap also confirmed the CD21_3 and CD21_4 to be fibroblast-like, with the

154 CD21_2 group showing an intermediate phenotype, distinct from the microglia cell types it was

155 clustered with (Fig. 3b). Taken together, the comparative analysis of the transcriptomic profiles

156 of our iMG and other cell types indicate that our iMG cells are indistinguishable from previously

157 reported iMG and adult/fetal MGLs at the transcriptomic level.

158

159 **iMG are enriched for AD GWAS loci, but lack enrichment of major neuropsychiatric**

160 **disease risk loci**

161 MGL have been implicated as a major cell type involved in AD disease progression [6-8].

162 However, whether hiPSC-derived iMG cells are also genetically relevant to AD has not

163 previously been evaluated. We first examined the expression similarity of a set of AD-

164 associated genes [17] between different cell types including our iMG (Fig. 4a). We found that

165 most AD risk genes showed similarly high level of expression in iMG and fetal/adult MGL, but

166 not in other non-MGL cell types. Hierarchical clustering using expression from these 31 genes

167 also showed that iMG cells were clustered together with fetal/adult MGL cells. As expected,

168 TREM2 expression is highly specific to iMG and fetal/adult MGL. APOE also shows highest

169 expression in iMG and MGL.

170

171 To further evaluate whether iMG is a relevant cell type for AD genetic risk, we used LDSC and

172 MAGMA [23-25] to partition heritability of AD GWAS loci near genes specifically expressed in

173 each cell type. This approach has been recently used to estimate disease risk enrichment for

174 each cell type based on genes expressed with high specificity [26], most notably in identifying

175 the schizophrenia-relevant neuronal cell types [27]. A normalized metric of cell type specificity of

176 gene expression was calculated for each gene using EWCE (Fig. 4b), and subsequently used to

177 rank genes for each cell type. In order to include a broad range of neural and immune cell types

178 that can help define cell type-specific expression, we incorporated additional single-cell RNA-

179 seq data [28] (Supplementary Table 3) to our current dataset and used replicates of bulk RNA-

180 seq for comparison. We found that the distributions of gene specificity values for bulk and

181 single-cell RNA-seq data were comparable, which suggests the normalization and filtering of

182 EWCE produced a cohesive dataset for LDSC and MAGMA analyses.

183

184 LDSC analysis of AD GWAS loci around the top 20% of genes (by specificity) found enrichment

185 for all MGL, microglia-like (MGL-like) cell types, and MCs (Fig. 4c); with single-cell RNA-Seq

186 MGL (scMGL) and aMGL further showing a similar enrichment regardless of sequencing

187 method. Consistent with a recent study showing genome-wide significant AD risk loci plausibly

188 operate in peripheral MC [29], we observed here that MC showed enrichment for AD risk similar

189 to that of the iMG cells (Fig. 4c, Supplementary Fig. 2). Using narrower gene windows of 20kb

190 and 50kb we observed even higher enrichment of our iMG Koz cell type than in Fig. 4 ($\alpha <$

191 0.004 in both instances), but chose the default 100kb window as it showed best enrichment

192 across all MGL and MGL-like cell types (See Supplementary Fig. 2 for details). For other tested

193 GWAS traits (SCZ; PD; MDD; BIP; ASD; Body Mass Index, BMI) (Fig. 4d), we observed

194 expected significant enrichment of SCZ and BIP GWAS signals in neurons (Neu) and a lesser

195 enrichment of PD, MDD and BMI GWAS loci. Oligodendrocytes (Olig) also showed a mild

196 enrichment for SCZ GWAS loci. Despite the known strong SCZ genetic risk factor complement

197 C4 (C4A) and its associated microglia function in abnormal synapse pruning [20], we did not

198 observe significant enrichment of SZ GWAS signals in iMG, MGL-like cell types, which is

199 consistent with a previous study [27]. Nor did we did not observe enrichment of GWAS signals

200   in iMG or MGL-like cell types for BMI and PD GWAS datasets, as expected due to no known

201   involvement of microglia.

202

203   We next evaluated the cell type-specific GWAS enrichment with a different tool, MAGMA. The

204   MAGMA cell typing method makes use of linear regression based on the specificity score,

205   allowing the use of all the expressed genes instead of a strict cutoff. Accordingly, we saw an

206   overall higher significance of enrichments in relevant cell types for AD and other GWAS trait

207   sets (Fig. 4d). MAGMA enrichments for AD achieved Bonferroni significance (α = 0.05 / 9

208   distinct cell types $\times$ 7 GWAS sets = 0.00079) for the MGL, MGL-like, and MC, cell types that

209   also showed strongest enrichment of AD loci with LDSC (Fig. 4c). As with LDSC, SCZ GWAS

210   loci were significantly enriched in Neu, but also had significant enrichment in Olig, astrocytes

211   (Ast) and NSC. MAGMA also gave a non-significant enrichment of AD in Ast, which was

212   undetected in LDSC (Fig. 4c). MAGMA showed enrichment of BMI loci in the Neu cell type

213   consistent with previous analysis [26], but also showed significant enrichment in NSC, Olig, Ast,

214   and endothelial cells (Fig. 4d). PD demonstrated a low level of enrichment across a majority of

215   these cell types without a significant cell type, similar to previous findings [27]. MDD and BIP

216   both showed significant enrichment of disease loci in neurons and oligodendrocytes, and with a

217   lesser significant enrichment in NSC, which are largely consistent with previous observations

218   [26,27]. It is noteworthy that for ASD that was not previously examined for genetically relevant

219   cell types, we found significant GWAS enrichment in neurons and oligodendrocytes. Taken

220   together, the results from LDSC and MAGMA analyses are overall consistent, showing

221   microglial-specific enrichment of preferentially gene expression of AD genetic risk loci, but not of

222   the risk loci of SZ and several other psychiatric disorders.

223

224   **Discussion**

225   Multiple attempts with a variety of methods have been made to derive iMG from hiPSCs with

226   mixed results [14-19]. We provide evidence that hiPSC-derived iMG share similar transcriptomic

227   profiles with aMGL and are genetically relevant to AD. Here, using a recently developed and a

228   simple protocol [19], we demonstrated its replicability by generating congruent results. The iMG

229   exhibited morphological and molecular characteristics of MGL and were transcriptionally

230   indistinguishable from aMGL. We further showed that iMG from hiPSCs and aMGL are similarly

231   enriched for common AD heritability, but not for SCZ or some other major psychiatric disease

232   risk GWAS loci, which has not been previously demonstrated.

233

234   AD is polygenic disorder, with possibly hundreds of risk genes each contributing a small

235   heritability. As a conceptual extension of the polygenic model, the omnigenic model for complex

236   disorders recently hypothesized most genes, if not all, expressed in a disease relevant cell type

237   may contribute to disease risk [30]. Thus, identifying a disease relevant cell type will be a key

238   step for dissecting the genetic causality for AD. Using two leading GWAS heritability partitioning

239   toolsets, we have shown that genes expressed in hiPSC-derived iMG were significantly

240   enriched for AD risk loci (Fig. 4c, d), with a significance level that was similar to that of multiple

241   other MGL sets and MC. Although heritability enrichment analysis is sensitive to some chosen

242   parameters such as the length of flanking genic regions and the metric of gene specificity

243   (Supplementary Fig. 2, 3), the overall cell type-specific enrichments of AD heritability agreed

244   across both methods, pointing to the comparable performance of iMG and MGL. The observed

245   shared enrichment pattern of AD heritability in iMG and MGL cell types was consistent with their

246   expression profiles for previously identified AD-associated genes (Fig. 4a). Taken together with

247   their overall transcriptomic similarity (Fig. 3), our results suggest that hiPSC-derived iMG cells

248   are a genetically relevant cellular model for studying genetic effects of AD risk factors.

249

250 Genetically relevant iMG can help to infer the putatively functional causal AD GWAS risk

251 variants and help elucidate their effects in a human cellular model. Because most AD GWAS

252 risk variants are in the noncoding part of the genome, putatively causal variants most likely

253 affect gene expression via altered chromatin accessibility to transcription factors, and

254 modification of regulatory regions. In this regard, open chromatin region (OCR) profiles of

255 hiPSC-derived iMG cells, like in hiPSC-derived excitatory neurons for SCZ, may help prioritize

256 the putatively functional GWAS risk variants that may alter chromatin accessibility and

257 transcriptional gene networks [31,32].

258

259 We acknowledge the limitations of our results. First, although we were able to replicate

260 Brownjohn's method [19], we also found that some differentiating iMG cultures develop

261 persistent fibroblast-like impurities of unclear origin, requiring careful screening of cultures to

262 prevent contamination. Second, given the cell lines used in this study were derived from

263 schizophrenic individuals, a potential concern is an inflated iMG enrichment for SCZ risk loci.

264 However, we found no evidence of this, suggesting the observed iMG enrichment for AD risk

265 loci was less likely to be confounded by using SCZ patient lines. Nonetheless, it would be ideal

266 to use cell lines derived from healthy control subjects for such cell type-specific enrichment

267 analyses for disease risk loci. Finally, although the iMG cells were transcriptionally

268 indistinguishable from primary aMGL cultured *in vitro*, that may not translate to functional

269 equivalence with primary microglia under *in vivo* conditions. Co-culture of iMGs with other types

270 of neurons or astrocytes in 2D culture or as part of brain organoids may further enhance the

271 validity of our *in vitro* model system.

272

273 The roles of MGL and the MGL-mediated neuroinflammation have been proposed in

274 neurodegenerative disorders such as AD [6,7] and PD [33,34]; and neuropsychiatric disorders

275 such as SCZ [20], BIP [35], MDD [36,37], and ASD [38]. Generating iMG that emulate aMGL,

276   either from hiPSC or from non-hiPSC cells [39], will have a broad impact by providing a

277   renewable source of iMG for basic and clinical studies. Although iMG were not found enriched

278   for major psychiatric genetic risk factors, these cells may remain to be a valuable cellular model

279   for testing specific pathogenic hypotheses: microglia-mediated abnormal synaptic pruning in

280   SCZ [20][21], and microglial activation in α-synuclein aggregation in PD [33]. And more recent

281   evidence [40,41] supports microglial crosstalk with astrocytes—which did show disease

282   enrichment across multiple disorders—a valuable future utility for advanced co-culture of

283   induced cell types. In summary, our demonstration of the genetic relevance of hiPSC-derived

284   iMG to AD offers support for iMG as an appropriate human cellular models for studying the

285   enigmatic causal mechanisms of AD and understanding the role of neuroinflammatory factors

286   in AD and other brain disorders, with the scalability to facilitate the development of more

287   effective therapeutics.

288

289 **Methods**

290 **hiPSC lines**

291 The two hiPSC lines, CD0000011 (CD11) and CD0000021 (CD21), were generated at RUCDR

292 NIMH Stem Cell Center from the cryopreserved lymphoblasts of Molecular Genetics Study of

293 Schizophrenia (MGS) [42] by using the non-integrating Sendai virus method. The two lines are

294 from schizophrenia cases, one male and the other female. The pluripotency of the hiPSC lines

295 was confirmed by immunofluorescence (IF) staining of pluripotency markers and by

296 Pluritest[43]. Confirmation of absence of chromosomal abnormality was performed by eSNP-

297 Karyotyping using RNA-seq data[44]. The NorthShore University HealthSystem Institutional

298 Review Board (IRB) approved the study.

299

300 **Derivation of PMPs and iMG**

301 CD11 and CD21 hiPSC lines were used to generated iMG by Brownjohn's method [19]. These

302 cell lines were cultured in mTeSR complete medium (85850, STEMCELL) with 2 ml daily media

303 changes. At least two days after passaging, hiPSCs were passaged to single cells and plated at

304 10,000 cells per well in 96-well round bottom ultra-low attachment plates (Corning) in 100 μl EB

305 media and plates were centrifuged at $300 \times$ g for 3 min. EB media was prepared by adding to

306 the complete mTeSR media BMP-4 (Thermofisher), SCF (Thermofisher), VEGF-121

307 (Peprotech), and ROCK inhibitor (Tocris). Cells were cultured for four days, with half media

308 change after two days. On day four, 16 EBs were plated on a 6-well plate and cultured in 3 ml

309 hematopoietic media with 2 ml media exchanges every five days. Hematopoietic media was

310 prepared by adding to the X-VIVO 15 (04-744Q, Lonza), GlutaMax (Thermofisher), Pen/strep

311 (Thermofisher), β-mercaptoethanol (Sigma), M-CSF (Thermofisher), and IL-3 (Thermofisher).

312 After five days culturing EBs in hematopoietic media, PMPs started to appear in the suspension

313 and were produced continuously in suspension for 34 days. After 10 days of culturing EBs,

314 PMPs could be harvested from suspension and plated in RPMI 1640 (Thermofisher) at 180,000

315 cells/cm^2 in 6- or 12-well plates. After one hour, PMPs adhered to surface and media was

316 changed to complete microglia media. Full media changes were done every 2 days. Complete

317 microglia media was prepared with RPMI 1640 by adding FBS (Thermofisher), Glutamax,

318 Pen/strep, IL-24 (PeptroTech), and GM-CSF (PeproTech). Final differentiation of PMPs into

319 microglia occurred over 6-10 days and cells could be kept for at least one month in this format.

320

321 **Phagocytosis of iMG**

322 To measure phagocytosis of bacterial particles, live imaging was performed on microglia

323 exposed to 50 µg/ml pHrodo red conjugated *E. coli* bioparticles (Invitrogen). As a positive

324 control for reduced phagocytosis, microglia were pre-treated (for 45 min) and co-treated with 10

325 µM of the actin polymerization inhibitor cytochalasin D. Live imaging was performed every 15

326 min after adding pHrodo-*E.coli* in order to assess phagocytosis kinetics. Area of pHrodo signal

327 in the fluorescent channel was measured and calculated as a proportion of total cell area

328 measured in the DIC channel.

329

330 **Immunofluorescence staining**

331 After washing cells in PBS, cell cultures were fixed in 4% (w/vol) paraformaldehyde and blocked

332 with 1% BSA, 0.3% (vol/vol) Triton-X100 in PBS before immunofluorescence staining. Primary

333 antibodies were TREM2 N-terminal (R&D Systems, 1:20), PU1 (Cell Signalling Technology,

334 1:100), and CD45 (Sigma, 1:200). Secondary antibodies were Alexa Fluor 488 chicken anti-goat

335 (ThermoFisher, 1:500) and Alexa Fluor 594 donkey anti-rabbit (Jackson ImmunoResearch,

336 1:1000).

337

338 **Quantitative (real-time) PCR and Bulk RNA-seq**

339   Quantitative RT-PCR was performed on total RNA from each stem cell line after PBS wash.

340   Cells were lysed in RLT plus buffer, and total RNA extracted with the RNeasy mini kit (Qiagen).

341   cDNA was reverse transcribed from RNA with a high-capacity cDNA reverse transcription kit

342   (Applied Biosystems). qPCR mix was prepared using Taqman Universal PCR master mix

343   (Applied Biosystems), TaqMan mRNA assays (Supplementary Table 1), and performed on a

344   Roche LightCycler 480. Total RNA was sent for sequencing to Novogene (en.novogene.com).

345   Sequencing libraries were prepared using the NEB Nextera kit with customized adapters. We

346   targeted the 25 M, 2×150 bp pair-end reads per sample.

347

348   **Transcriptomic Analysis**

349   SRA archived raw sequencing reads were downloaded for NCBI Bioprojects (PRJNA350562,

350   PRJNA435266, PRJEB22885, PRJNA496431) [15,19,45,46] and processed alongside our

351   sample reads. Reads were trimmed with Trimmomatic v0.36 [47] and mapped using STAR

352   2.6.1d [48]. Fragment counts were generated with featureCounts 1.6.3 [49]. Gene information

353   was collected from biomaRt 2.38.0 [50], and 19,951 protein-coding genes with GC content

354   information were used for downstream analysis. Overall principal component analysis utilized

355   cqn 1.28.1 [51] for normalization and a minimum expression filter of at least 1 cpm in at least 3

356   samples, applied with edgeR 3.24.3 [52] resulting in a comparison set of 15,469 genes. The

357   expression heatmap subset of genes AD relevant genes, defined in Haenseler et al. [17], is

358   derived from this normalized set. Pairwise sample distances were calculated from raw protein-

359   coding gene counts using Poisson distance with PoiClaClu 1.0.2.1 [53].

360

361   **Cell Type Specificity**

362   Additional human neural cell data was gathered from Darmanis et al. [28] and merged with raw

363   protein coding counts from above to generate a shared set of genes. Cell type specificity was

364   generated for each sample set with EWCE 0.99.2 [54], after first removing sporadic expression

365 with ANOVA analysis. Given the cell type similarity of all microglia and PMP sample sets (MGL-

366 like sets), each of these seven sets was individually compared to all non-MGL-like sets, for a

367 total of seven 9-sample specificity matrices. After examination, of specificity distributions and

368 MAGMA 1.07b [23] enrichment results, it was decided that enrichment values for non-MGL-like

369 sets were comparable regardless of which MGL-like set they were tested against

370 (Supplementary Fig. 3). For continuing analysis, the non-MGL-like specificity values when

371 compared against primary adult microglia were chosen to generate gene sets for LDSC.

372

Cell Type GWAS Enrichment Using MAGMA and LDSC

374 MAGMA enrichment was conducted with the MAGMA Celltyping R package [27] (see URLs)

375 using the specificity values above. Gene-level association statistics were tested with window

376 sizes of 100kb (50kb upstream, 50kb downstream), 57.5kb (50kb upstream, 7.5kb downstream),

377 and the recommended 11.5 kb window (10kb upstream, 1.5kb downstream). The recommended

378 window provided the best overall enrichment across all MGL-like cell types. GWAS datasets

379 (Supplementary Table 4) for Alzheimer's disease [6], Parkinson's disease [55], Schizophrenia

380 [56], major depressive disorder [57], bipolar disorder [58], autism spectrum disorder [59], and

381 Body Mass Index [60] were run for each of the above 9-sample specificity matrices

382 (Supplementary Fig. 3).

383

384 LDSC 1.0.0 [24,25] analysis was conducted using gene sets derived from gene specificity

385 values for each of the fifteen different cell types. Top percentile by specificity was checked at

386 10%, 20%, 30%, 40%, and 50% for all GWAS sets. Gene annotation files were constructed with

387 the recommended 100kb window using the 1000 Genomes Project phase 3 [61] data provided

388 in the LDSC wiki guide (see URLs). The LDSC partitions were built with the recommended

389 settings for a 1-cM window and HapMap3 limited SNPs. For regression, the baseline LD scores

390 for 1000 Genomes Phase 3 version 2.2 were used with the provided HapMap3 SNP LD

391   weights, and the 'overlap-annot' argument was used with the 1000 Genomes phase 3 minor-

392   allele frequency files. The top 20% of genes provided the best overall enrichment across all

393   MGL-like cell types and were used for figures (for all percentiles see Supplementary Fig. 2).

394

395   **Accession number**

396   Expression data for the iMG generated in this study have been submitted to the GEO database:

397   GSE129630.

398

399   **Supplementary information**

400   Supplementary Tables 1-4 and Supplementary Figures 1-3

401

402   **URLs**

403   LDSC method: https://github.com/bulik/ldsc/wiki/Cell-type-specific-analyses; MAGMA:

404   https://ctg.cncr.nl/software/magma; MAGMA Celltyping:

405   https://github.com/NathanSkene/MAGMA_Celltyping; R: https://cran.r-project.org/; scripts used

406   to process data, including software options available at:

407   https://rbutleriii.github.io/center_for_psychiatric_genomics

408

References

409

410   1   Hardy J, Selkoe DJ: The amyloid hypothesis of Alzheimer's disease: progress and
411   problems on the road to therapeutics. Science 2002;297:353-356.
412   2   Hollingworth P, Harold D, Sims R, Gerrish A, Lambert JC, Carrasquillo MM, Abraham R,
413   Hamshere ML, Pahwa JS, Moskvina V, Dowzell K, Jones N, Stretton A, Thomas C, Richards A,
414   Ivanov D, Widdowson C, Chapman J, Lovestone S, Powell J, Proitsi P, Lupton MK, Brayne C,
415   Rubinsztein DC, Gill M, Lawlor B, Lynch A, Brown KS, Passmore PA, Craig D, McGuinness B, Todd
416   S, Holmes C, Mann D, Smith AD, Beaumont H, Warden D, Wilcock G, Love S, Kehoe PG, Hooper
417   NM, Vardy ER, Hardy J, Mead S, Fox NC, Rossor M, Collinge J, Maier W, Jessen F, Ruther E,
418   Schurmann B, Heun R, Kolsch H, van den Bussche H, Heuser I, Kornhuber J, Wiltfang J, Dichgans
419   M, Frolich L, Hampel H, Gallacher J, Hull M, Rujescu D, Giegling I, Goate AM, Kauwe JS,
420   Cruchaga C, Nowotny P, Morris JC, Mayo K, Sleegers K, Bettens K, Engelborghs S, De Deyn PP,
421   Van Broeckhoven C, Livingston G, Bass NJ, Gurling H, McQuillin A, Gwilliam R, Deloukas P, Al-
422   Chalabi A, Shaw CE, Tsolaki M, Singleton AB, Guerreiro R, Muhleisen TW, Nothen MM, Moebus
423   S, Jockel KH, Klopp N, Wichmann HE, Pankratz VS, Sando SB, Aasly JO, Barcikowska M, Wszolek
424   ZK, Dickson DW, Graff-Radford NR, Petersen RC, Alzheimer's Disease Neuroimaging I, van Duijn
425   CM, Breteler MM, Ikram MA, DeStefano AL, Fitzpatrick AL, Lopez O, Launer LJ, Seshadri S,
426   consortium C, Berr C, Campion D, Epelbaum J, Dartigues JF, Tzourio C, Alperovitch A, Lathrop M,
427   consortium E, Feulner TM, Friedrich P, Riehle C, Krawczak M, Schreiber S, Mayhaus M,
428   Nicolhaus S, Wagenpfeil S, Steinberg S, Stefansson H, Stefansson K, Snaedal J, Bjornsson S,
429   Jonsson PV, Chouraki V, Genier-Boley B, Hiltunen M, Soininen H, Combarros O, Zelenika D,
430   Delepine M, Bullido MJ, Pasquier F, Mateo I, Frank-Garcia A, Porcellini E, Hanon O, Coto E,
431   Alvarez V, Bosco P, Siciliano G, Mancuso M, Panza F, Solfrizzi V, Nacmias B, Sorbi S, Bossu P,
432   Piccardi P, Arosio B, Annoni G, Seripa D, Pilotto A, Scarpini E, Galimberti D, Brice A, Hannequin
433   D, Licastro F, Jones L, Holmans PA, Jonsson T, Riemenschneider M, Morgan K, Younkin SG,
434   Owen MJ, O'Donovan M, Amouyel P, Williams J: Common variants at ABCA7, MS4A6A/MS4A4E,
435   EPHA1, CD33 and CD2AP are associated with Alzheimer's disease. Nat Genet 2011;43:429-435.
436   3   Naj AC, Jun G, Beecham GW, Wang LS, Vardarajan BN, Buros J, Gallins PJ, Buxbaum JD,
437   Jarvik GP, Crane PK, Larson EB, Bird TD, Boeve BF, Graff-Radford NR, De Jager PL, Evans D,
438   Schneider JA, Carrasquillo MM, Ertekin-Taner N, Younkin SG, Cruchaga C, Kauwe JS, Nowotny P,
439   Kramer P, Hardy J, Huentelman MJ, Myers AJ, Barmada MM, Demirci FY, Baldwin CT, Green RC,
440   Rogaeva E, St George-Hyslop P, Arnold SE, Barber R, Beach T, Bigio EH, Bowen JD, Boxer A,
441   Burke JR, Cairns NJ, Carlson CS, Carney RM, Carroll SL, Chui HC, Clark DG, Corneveaux J, Cotman
442   CW, Cummings JL, DeCarli C, DeKosky ST, Diaz-Arrastia R, Dick M, Dickson DW, Ellis WG, Faber
443   KM, Fallon KB, Farlow MR, Ferris S, Frosch MP, Galasko DR, Ganguli M, Gearing M, Geschwind
444   DH, Ghetti B, Gilbert JR, Gilman S, Giordani B, Glass JD, Growdon JH, Hamilton RL, Harrell LE,
445   Head E, Honig LS, Hulette CM, Hyman BT, Jicha GA, Jin LW, Johnson N, Karlawish J, Karydas A,
446   Kaye JA, Kim R, Koo EH, Kowall NW, Lah JJ, Levey AI, Lieberman AP, Lopez OL, Mack WJ, Marson
447   DC, Martiniuk F, Mash DC, Masliah E, McCormick WC, McCurry SM, McDavid AN, McKee AC,
448   Mesulam M, Miller BL, Miller CA, Miller JW, Parisi JE, Perl DP, Peskind E, Petersen RC, Poon
449   WW, Quinn JF, Rajbhandary RA, Raskind M, Reisberg B, Ringman JM, Roberson ED, Rosenberg
450   RN, Sano M, Schneider LS, Seeley W, Shelanski ML, Slifer MA, Smith CD, Sonnen JA, Spina S,
451   Stern RA, Tanzi RE, Trojanowski JQ, Troncoso JC, Van Deerlin VM, Vinters HV, Vonsattel JP,

452 Weintraub S, Welsh-Bohmer KA, Williamson J, Woltjer RL, Cantwell LB, Dombroski BA, Beekly D,
453 Lunetta KL, Martin ER, Kamboh MI, Saykin AJ, Reiman EM, Bennett DA, Morris JC, Montine TJ,
454 Goate AM, Blacker D, Tsuang DW, Hakonarson H, Kukull WA, Foroud TM, Haines JL, Mayeux R,
455 Pericak-Vance MA, Farrer LA, Schellenberg GD: Common variants at MS4A4/MS4A6E, CD2AP,
456 CD33 and EPHA1 are associated with late-onset Alzheimer's disease. Nat Genet 2011;43:436-
457 441.
458 4   Karch CM, Goate AM: Alzheimer's disease risk genes and mechanisms of disease
459 pathogenesis. Biol Psychiatry 2015;77:43-51.
460 5   Lambert JC, Ibrahim-Verbaas CA, Harold D, Naj AC, Sims R, Bellenguez C, DeStafano AL,
461 Bis JC, Beecham GW, Grenier-Boley B, Russo G, Thorton-Wells TA, Jones N, Smith AV, Chouraki
462 V, Thomas C, Ikram MA, Zelenika D, Vardarajan BN, Kamatani Y, Lin CF, Gerrish A, Schmidt H,
463 Kunkle B, Dunstan ML, Ruiz A, Bihoreau MT, Choi SH, Reitz C, Pasquier F, Cruchaga C, Craig D,
464 Amin N, Berr C, Lopez OL, De Jager PL, Deramecourt V, Johnston JA, Evans D, Lovestone S,
465 Letenneur L, Moron FJ, Rubinsztein DC, Eiriksdottir G, Sleegers K, Goate AM, Fievet N,
466 Huentelman MW, Gill M, Brown K, Kamboh MI, Keller L, Barberger-Gateau P, McGuiness B,
467 Larson EB, Green R, Myers AJ, Dufouil C, Todd S, Wallon D, Love S, Rogaeva E, Gallacher J, St
468 George-Hyslop P, Clarimon J, Lleo A, Bayer A, Tsuang DW, Yu L, Tsolaki M, Bossu P, Spalletta G,
469 Proitsi P, Collinge J, Sorbi S, Sanchez-Garcia F, Fox NC, Hardy J, Deniz Naranjo MC, Bosco P,
470 Clarke R, Brayne C, Galimberti D, Mancuso M, Matthews F, European Alzheimer's Disease I,
471 Genetic, Environmental Risk in Alzheimer's D, Alzheimer's Disease Genetic C, Cohorts for H,
472 Aging Research in Genomic E, Moebus S, Mecocci P, Del Zompo M, Maier W, Hampel H, Pilotto
473 A, Bullido M, Panza F, Caffarra P, Nacmias B, Gilbert JR, Mayhaus M, Lannefelt L, Hakonarson H,
474 Pichler S, Carrasquillo MM, Ingelsson M, Beekly D, Alvarez V, Zou F, Valladares O, Younkin SG,
475 Coto E, Hamilton-Nelson KL, Gu W, Razquin C, Pastor P, Mateo I, Owen MJ, Faber KM, Jonsson
476 PV, Combarros O, O'Donovan MC, Cantwell LB, Soininen H, Blacker D, Mead S, Mosley TH, Jr.,
477 Bennett DA, Harris TB, Fratiglioni L, Holmes C, de Bruijn RF, Passmore P, Montine TJ, Bettens K,
478 Rotter JI, Brice A, Morgan K, Foroud TM, Kukull WA, Hannequin D, Powell JF, Nalls MA, Ritchie
479 K, Lunetta KL, Kauwe JS, Boerwinkle E, Riemenschneider M, Boada M, Hiltuenen M, Martin ER,
480 Schmidt R, Rujescu D, Wang LS, Dartigues JF, Mayeux R, Tzourio C, Hofman A, Nothen MM,
481 Graff C, Psaty BM, Jones L, Haines JL, Holmans PA, Lathrop M, Pericak-Vance MA, Launer LJ,
482 Farrer LA, van Duijn CM, Van Broeckhoven C, Moskvina V, Seshadri S, Williams J, Schellenberg
483 GD, Amouyel P: Meta-analysis of 74,046 individuals identifies 11 new susceptibility loci for
484 Alzheimer's disease. Nat Genet 2013;45:1452-1458.
485 6   Jansen IE, Savage JE, Watanabe K, Bryois J, Williams DM, Steinberg S, Sealock J, Karlsson
486 IK, Hagg S, Athanasiu L, Voyle N, Proitsi P, Witoelar A, Stringer S, Aarsland D, Almdahl IS,
487 Andersen F, Bergh S, Bettella F, Bjornsson S, Braekhus A, Brathen G, de Leeuw C, Desikan RS,
488 Djurovic S, Dumitrescu L, Fladby T, Hohman TJ, Jonsson PV, Kiddle SJ, Rongve A, Saltvedt I,
489 Sando SB, Selbaek G, Shoai M, Skene NG, Snaedal J, Stordal E, Ulstein ID, Wang Y, White LR,
490 Hardy J, Hjerling-Leffler J, Sullivan PF, van der Flier WM, Dobson R, Davis LK, Stefansson H,
491 Stefansson K, Pedersen NL, Ripke S, Andreassen OA, Posthuma D: Genome-wide meta-analysis
492 identifies new loci and functional pathways influencing Alzheimer's disease risk. Nat Genet
493 2019;51:404-413.
494 7   Sims R, van der Lee SJ, Naj AC, Bellenguez C, Badarinarayan N, Jakobsdottir J, Kunkle
495 BW, Boland A, Raybould R, Bis JC, Martin ER, Grenier-Boley B, Heilmann-Heimbach S, Chouraki

496 V, Kuzma AB, Sleegers K, Vronskaya M, Ruiz A, Graham RR, Olaso R, Hoffmann P, Grove ML,
497 Vardarajan BN, Hiltunen M, Nothen MM, White CC, Hamilton-Nelson KL, Epelbaum J, Maier W,
498 Choi SH, Beecham GW, Dulary C, Herms S, Smith AV, Funk CC, Derbois C, Forstner AJ, Ahmad S,
499 Li H, Bacq D, Harold D, Satizabal CL, Valladares O, Squassina A, Thomas R, Brody JA, Qu L,
500 Sanchez-Juan P, Morgan T, Wolters FJ, Zhao Y, Garcia FS, Denning N, Fornage M, Malamon J,
501 Naranjo MCD, Majounie E, Mosley TH, Dombroski B, Wallon D, Lupton MK, Dupuis J, Whitehead
502 P, Fratiglioni L, Medway C, Jian X, Mukherjee S, Keller L, Brown K, Lin H, Cantwell LB, Panza F,
503 McGuinness B, Moreno-Grau S, Burgess JD, Solfrizzi V, Proitsi P, Adams HH, Allen M, Seripa D,
504 Pastor P, Cupples LA, Price ND, Hannequin D, Frank-Garcia A, Levy D, Chakrabarty P, Caffarra P,
505 Giegling I, Beiser AS, Giedraitis V, Hampel H, Garcia ME, Wang X, Lannfelt L, Mecocci P,
506 Eiriksdottir G, Crane PK, Pasquier F, Boccardi V, Henandez I, Barber RC, Scherer M, Tarraga L,
507 Adams PM, Leber M, Chen Y, Albert MS, Riedel-Heller S, Emilsson V, Beekly D, Braae A, Schmidt
508 R, Blacker D, Masullo C, Schmidt H, Doody RS, Spalletta G, Longstreth WT, Jr., Fairchild TJ, Bossu
509 P, Lopez OL, Frosch MP, Sacchinelli E, Ghetti B, Yang Q, Huebinger RM, Jessen F, Li S, Kamboh
510 MI, Morris J, Sotolongo-Grau O, Katz MJ, Corcoran C, Dunstan M, Braddel A, Thomas C, Meggy
511 A, Marshall R, Gerrish A, Chapman J, Aguilar M, Taylor S, Hill M, Fairen MD, Hodges A, Vellas B,
512 Soininen H, Kloszewska I, Daniilidou M, Uphill J, Patel Y, Hughes JT, Lord J, Turton J, Hartmann
513 AM, Cecchetti R, Fenoglio C, Serpente M, Arcaro M, Caltagirone C, Orfei MD, Ciaramella A,
514 Pichler S, Mayhaus M, Gu W, Lleo A, Fortea J, Blesa R, Barber IS, Brookes K, Cupidi C, Maletta
515 RG, Carrell D, Sorbi S, Moebus S, Urbano M, Pilotto A, Kornhuber J, Bosco P, Todd S, Craig D,
516 Johnston J, Gill M, Lawlor B, Lynch A, Fox NC, Hardy J, Consortium A, Albin RL, Apostolova LG,
517 Arnold SE, Asthana S, Atwood CS, Baldwin CT, Barnes LL, Barral S, Beach TG, Becker JT, Bigio EH,
518 Bird TD, Boeve BF, Bowen JD, Boxer A, Burke JR, Burns JM, Buxbaum JD, Cairns NJ, Cao C,
519 Carlson CS, Carlsson CM, Carney RM, Carrasquillo MM, Carroll SL, Diaz CC, Chui HC, Clark DG,
520 Cribbs DH, Crocco EA, DeCarli C, Dick M, Duara R, Evans DA, Faber KM, Fallon KB, Fardo DW,
521 Farlow MR, Ferris S, Foroud TM, Galasko DR, Gearing M, Geschwind DH, Gilbert JR, Graff-
522 Radford NR, Green RC, Growdon JH, Hamilton RL, Harrell LE, Honig LS, Huentelman MJ, Hulette
523 CM, Hyman BT, Jarvik GP, Abner E, Jin LW, Jun G, Karydas A, Kaye JA, Kim R, Kowall NW, Kramer
524 JH, LaFerla FM, Lah JJ, Leverenz JB, Levey AI, Li G, Lieberman AP, Lunetta KL, Lyketsos CG,
525 Marson DC, Martiniuk F, Mash DC, Masliah E, McCormick WC, McCurry SM, McDavid AN,
526 McKee AC, Mesulam M, Miller BL, Miller CA, Miller JW, Morris JC, Murrell JR, Myers AJ,
527 O'Bryant S, Olichney JM, Pankratz VS, Parisi JE, Paulson HL, Perry W, Peskind E, Pierce A, Poon
528 WW, Potter H, Quinn JF, Raj A, Raskind M, Reisberg B, Reitz C, Ringman JM, Roberson ED,
529 Rogaeva E, Rosen HJ, Rosenberg RN, Sager MA, Saykin AJ, Schneider JA, Schneider LS, Seeley
530 WW, Smith AG, Sonnen JA, Spina S, Stern RA, Swerdlow RH, Tanzi RE, Thornton-Wells TA,
531 Trojanowski JQ, Troncoso JC, Van Deerlin VM, Van Eldik LJ, Vinters HV, Vonsattel JP, Weintraub
532 S, Welsh-Bohmer KA, Wilhelmsen KC, Williamson J, Wingo TS, Woltjer RL, Wright CB, Yu CE, Yu
533 L, Garzia F, Golamaully F, Septier G, Engelborghs S, Vandenberghe R, De Deyn PP, Fernadez CM,
534 Benito YA, Thonberg H, Forsell C, Lilius L, Kinhult-Stahlbom A, Kilander L, Brundin R, Concari L,
535 Helisalmi S, Koivisto AM, Haapasalo A, Dermecourt V, Fievet N, Hanon O, Dufouil C, Brice A,
536 Ritchie K, Dubois B, Himali JJ, Keene CD, Tschanz J, Fitzpatrick AL, Kukull WA, Norton M,
537 Aspelund T, Larson EB, Munger R, Rotter JI, Lipton RB, Bullido MJ, Hofman A, Montine TJ, Coto
538 E, Boerwinkle E, Petersen RC, Alvarez V, Rivadeneira F, Reiman EM, Gallo M, O'Donnell CJ,
539 Reisch JS, Bruni AC, Royall DR, Dichgans M, Sano M, Galimberti D, St George-Hyslop P, Scarpini

540   E, Tsuang DW, Mancuso M, Bonuccelli U, Winslow AR, Daniele A, Wu CK, Gerad/Perades CAE,
541   Peters O, Nacmias B, Riemenschneider M, Heun R, Brayne C, Rubinsztein DC, Bras J, Guerreiro
542   R, Al-Chalabi A, Shaw CE, Collinge J, Mann D, Tsolaki M, Clarimon J, Sussams R, Lovestone S,
543   O'Donovan MC, Owen MJ, Behrens TW, Mead S, Goate AM, Uitterlinden AG, Holmes C,
544   Cruchaga C, Ingelsson M, Bennett DA, Powell J, Golde TE, Graff C, De Jager PL, Morgan K,
545   Ertekin-Taner N, Combarros O, Psaty BM, Passmore P, Younkin SG, Berr C, Gudnason V, Rujescu
546   D, Dickson DW, Dartigues JF, DeStefano AL, Ortega-Cubero S, Hakonarson H, Campion D, Boada
547   M, Kauwe JK, Farrer LA, Van Broeckhoven C, Ikram MA, Jones L, Haines JL, Tzourio C, Launer LJ,
548   Escott-Price V, Mayeux R, Deleuze JF, Amin N, Holmans PA, Pericak-Vance MA, Amouyel P, van
549   Duijn CM, Ramirez A, Wang LS, Lambert JC, Seshadri S, Williams J, Schellenberg GD: Rare coding
550   variants in PLCG2, ABI3, and TREM2 implicate microglial-mediated innate immunity in
551   Alzheimer's disease. Nat Genet 2017;49:1373-1384.
552   8   Keren-Shaul H, Spinrad A, Weiner A, Matcovitch-Natan O, Dvir-Szternfeld R, Ulland TK,
553   David E, Baruch K, Lara-Astaiso D, Toth B, Itzkovitz S, Colonna M, Schwartz M, Amit I: A Unique
554   Microglia Type Associated with Restricting Development of Alzheimer's Disease. Cell
555   2017;169:1276-1290 e1217.
556   9   Galatro TF, Holtman IR, Lerario AM, Vainchtein ID, Brouwer N, Sola PR, Veras MM,
557   Pereira TF, Leite REP, Moller T, Wes PD, Sogayar MC, Laman JD, den Dunnen W, Pasqualucci CA,
558   Oba-Shinjo SM, Boddeke E, Marie SKN, Eggen BJL: Transcriptomic analysis of purified human
559   cortical microglia reveals age-associated changes. Nat Neurosci 2017;20:1162-1171.
560   10   Kierdorf K, Erny D, Goldmann T, Sander V, Schulz C, Perdiguero EG, Wieghofer P,
561   Heinrich A, Riemke P, Holscher C, Muller DN, Luckow B, Brocker T, Debowski K, Fritz G,
562   Opdenakker G, Diefenbach A, Biber K, Heikenwalder M, Geissmann F, Rosenbauer F, Prinz M:
563   Microglia emerge from erythromyeloid precursors via Pu.1- and Irf8-dependent pathways. Nat
564   Neurosci 2013;16:273-280.
565   11   Ginhoux F, Greter M, Leboeuf M, Nandi S, See P, Gokhan S, Mehler MF, Conway SJ, Ng
566   LG, Stanley ER, Samokhvalov IM, Merad M: Fate mapping analysis reveals that adult microglia
567   derive from primitive macrophages. Science 2010;330:841-845.
568   12   Prinz M, Priller J: Microglia and brain macrophages in the molecular age: from origin to
569   neuropsychiatric disease. Nat Rev Neurosci 2014;15:300-312.
570   13   Nayak D, Roth TL, McGavern DB: Microglia development and function. Annu Rev
571   Immunol 2014;32:367-402.
572   14   Muffat J, Li Y, Yuan B, Mitalipova M, Omer A, Corcoran S, Bakiasi G, Tsai LH, Aubourg P,
573   Ransohoff RM, Jaenisch R: Efficient derivation of microglia-like cells from human pluripotent
574   stem cells. Nat Med 2016;22:1358-1367.
575   15   Abud EM, Ramirez RN, Martinez ES, Healy LM, Nguyen CHH, Newman SA, Yeromin AV,
576   Scarfone VM, Marsh SE, Fimbres C, Caraway CA, Fote GM, Madany AM, Agrawal A, Kayed R,
577   Gylys KH, Cahalan MD, Cummings BJ, Antel JP, Mortazavi A, Carson MJ, Poon WW, Blurton-
578   Jones M: iPSC-Derived Human Microglia-like Cells to Study Neurological Diseases. Neuron
579   2017;94:278-293 e279.
580   16   Douvaras P, Sun B, Wang M, Kruglikov I, Lallos G, Zimmer M, Terrenoire C, Zhang B,
581   Gandy S, Schadt E, Freytes DO, Noggle S, Fossati V: Directed Differentiation of Human
582   Pluripotent Stem Cells to Microglia. Stem cell reports 2017;8:1516-1524.

583   17   Haenseler W, Sansom SN, Buchrieser J, Newey SE, Moore CS, Nicholls FJ, Chintawar S,
584   Schnell C, Antel JP, Allen ND, Cader MZ, Wade-Martins R, James WS, Cowley SA: A Highly
585   Efficient Human Pluripotent Stem Cell Microglia Model Displays a Neuronal-Co-culture-Specific
586   Expression Profile and Inflammatory Response. Stem cell reports 2017;8:1727-1742.
587   18   Pandya H, Shen MJ, Ichikawa DM, Sedlock AB, Choi Y, Johnson KR, Kim G, Brown MA,
588   Elkahloun AG, Maric D, Sweeney CL, Gossa S, Malech HL, McGavern DB, Park JK: Differentiation
589   of human and murine induced pluripotent stem cells to microglia-like cells. Nat Neurosci
590   2017;20:753-759.
591   19   Brownjohn PW, Smith J, Solanki R, Lohmann E, Houlden H, Hardy J, Dietmann S, Livesey
592   FJ: Functional Studies of Missense TREM2 Mutations in Human Stem Cell-Derived Microglia.
593   Stem cell reports 2018;10:1294-1307.
594   20   Sekar A, Bialas AR, de Rivera H, Davis A, Hammond TR, Kamitaki N, Tooley K, Presumey J,
595   Baum M, Van Doren V, Genovese G, Rose SA, Handsaker RE, Daly MJ, Carroll MC, Stevens B,
596   McCarroll SA: Schizophrenia risk from complex variation of complement component 4. Nature
597   2016;530:177-183.
598   21   Sellgren CM, Gracias J, Watmuff B, Biag JD, Thanos JM, Whittredge PB, Fu T, Worringer
599   K, Brown HE, Wang J, Kaykas A, Karmacharya R, Goold CP, Sheridan SD, Perlis RH: Increased
600   synapse elimination by microglia in schizophrenia patient-derived models of synaptic pruning.
601   Nat Neurosci 2019;22:374-385.
602   22   Bachiller S, Jimenez-Ferrer I, Paulus A, Yang Y, Swanberg M, Deierborg T, Boza-Serrano
603   A: Microglia in Neurological Diseases: A Road Map to Brain-Disease Dependent-Inflammatory
604   Response. Front Cell Neurosci 2018;12:488.
605   23   de Leeuw CA, Mooij JM, Heskes T, Posthuma D: MAGMA: generalized gene-set analysis
606   of GWAS data. PLoS Comput Biol 2015;11:e1004219.
607   24   Bulik-Sullivan BK, Loh PR, Finucane HK, Ripke S, Yang J, Schizophrenia Working Group of
608   the Psychiatric Genomics C, Patterson N, Daly MJ, Price AL, Neale BM: LD Score regression
609   distinguishes confounding from polygenicity in genome-wide association studies. Nat Genet
610   2015;47:291-295.
611   25   Finucane HK, Bulik-Sullivan B, Gusev A, Trynka G, Reshef Y, Loh PR, Anttila V, Xu H, Zang
612   C, Farh K, Ripke S, Day FR, ReproGen C, Schizophrenia Working Group of the Psychiatric
613   Genomics C, Consortium R, Purcell S, Stahl E, Lindstrom S, Perry JR, Okada Y, Raychaudhuri S,
614   Daly MJ, Patterson N, Neale BM, Price AL: Partitioning heritability by functional annotation
615   using genome-wide association summary statistics. Nat Genet 2015;47:1228-1235.
616   26   Finucane HK, Reshef YA, Anttila V, Slowikowski K, Gusev A, Byrnes A, Gazal S, Loh PR,
617   Lareau C, Shoresh N, Genovese G, Saunders A, Macosko E, Pollack S, Brainstorm C, Perry JRB,
618   Buenrostro JD, Bernstein BE, Raychaudhuri S, McCarroll S, Neale BM, Price AL: Heritability
619   enrichment of specifically expressed genes identifies disease-relevant tissues and cell types. Nat
620   Genet 2018;50:621-629.
621   27   Skene NG, Bryois J, Bakken TE, Breen G, Crowley JJ, Gaspar HA, Giusti-Rodriguez P,
622   Hodge RD, Miller JA, Munoz-Manchado AB, O'Donovan MC, Owen MJ, Pardinas AF, Ryge J,
623   Walters JTR, Linnarsson S, Lein ES, Major Depressive Disorder Working Group of the Psychiatric
624   Genomics C, Sullivan PF, Hjerling-Leffler J: Genetic identification of brain cell types underlying
625   schizophrenia. Nat Genet 2018;50:825-833.

626 28   Darmanis S, Sloan SA, Zhang Y, Enge M, Caneda C, Shuer LM, Hayden Gephart MG,
627 Barres BA, Quake SR: A survey of human brain transcriptome diversity at the single cell level.
628 Proc Natl Acad Sci U S A 2015;112:7285-7290.
629 29   Tansey KE, Cameron D, Hill MJ: Genetic risk for Alzheimer's disease is concentrated in
630 specific macrophage and microglial transcriptional networks. Genome Med 2018;10:14.
631 30   Boyle EA, Li YI, Pritchard JK: An Expanded View of Complex Traits: From Polygenic to
632 Omnigenic. Cell 2017;169:1177-1186.
633 31   Forrest MP, Zhang H, Moy W, McGowan H, Leites C, Dionisio LE, Xu Z, Shi J, Sanders AR,
634 Greenleaf WJ, Cowan CA, Pang ZP, Gejman PV, Penzes P, Duan J: Open Chromatin Profiling in
635 hiPSC-Derived Neurons Prioritizes Functional Noncoding Psychiatric Risk Variants and Highlights
636 Neurodevelopmental Loci. Cell Stem Cell 2017;21:305-318 e308.
637 32   Zhang S, Moy W, Zhang H, Leites C, McGowan H, Shi J, Sanders AR, Pang ZP, Gejman PV,
638 Duan J: Open chromatin dynamics reveals stage-specific transcriptional networks in hiPSC-
639 based neurodevelopmental model. Stem Cell Res 2018;29:88-98.
640 33   Sampson TR, Debelius JW, Thron T, Janssen S, Shastri GG, Ilhan ZE, Challis C, Schretter
641 CE, Rocha S, Gradinaru V, Chesselet MF, Keshavarzian A, Shannon KM, Krajmalnik-Brown R,
642 Wittung-Stafshede P, Knight R, Mazmanian SK: Gut Microbiota Regulate Motor Deficits and
643 Neuroinflammation in a Model of Parkinson's Disease. Cell 2016;167:1469-1480 e1412.
644 34   Hirsch EC, Hunot S: Neuroinflammation in Parkinson's disease: a target for
645 neuroprotection? The Lancet Neurology 2009;8:382-397.
646 35   Haarman BC, Riemersma-Van der Lek RF, de Groot JC, Ruhe HG, Klein HC, Zandstra TE,
647 Burger H, Schoevers RA, de Vries EF, Drexhage HA, Nolen WA, Doorduin J: Neuroinflammation
648 in bipolar disorder - A [(11)C]-(R)-PK11195 positron emission tomography study. Brain Behav
649 Immun 2014;40:219-225.
650 36   Hurley LL, Tizabi Y: Neuroinflammation, neurodegeneration, and depression. Neurotox
651 Res 2013;23:131-144.
652 37   Tang MM, Lin WJ, Pan YQ, Li YC: Fibroblast Growth Factor 2 Modulates Hippocampal
653 Microglia Activation in a Neuroinflammation Induced Model of Depression. Front Cell Neurosci
654 2018;12:255.
655 38   Suzuki K, Sugihara G, Ouchi Y, Nakamura K, Futatsubashi M, Takebayashi K, Yoshihara Y,
656 Omata K, Matsumoto K, Tsuchiya KJ, Iwata Y, Tsujii M, Sugiyama T, Mori N: Microglial activation
657 in young adults with autism spectrum disorder. JAMA Psychiatry 2013;70:49-58.
658 39   Sellgren CM, Sheridan SD, Gracias J, Xuan D, Fu T, Perlis RH: Patient-specific models of
659 microglia-mediated engulfment of synapses and neural progenitors. Mol Psychiatry
660 2017;22:170-177.
661 40   Rothhammer V, Borucki DM, Tjon EC, Takenaka MC, Chao CC, Ardura-Fabregat A, de
662 Lima KA, Gutierrez-Vazquez C, Hewson P, Staszewski O, Blain M, Healy L, Neziraj T, Borio M,
663 Wheeler M, Dragin LL, Laplaud DA, Antel J, Alvarez JI, Prinz M, Quintana FJ: Microglial control of
664 astrocytes in response to microbial metabolites. Nature 2018;557:724-728.
665 41   Liddelow SA, Guttenplan KA, Clarke LE, Bennett FC, Bohlen CJ, Schirmer L, Bennett ML,
666 Munch AE, Chung WS, Peterson TC, Wilton DK, Frouin A, Napier BA, Panicker N, Kumar M,
667 Buckwalter MS, Rowitch DH, Dawson VL, Dawson TM, Stevens B, Barres BA: Neurotoxic reactive
668 astrocytes are induced by activated microglia. Nature 2017;541:481-487.

669   42   Shi J, Levinson DF, Duan J, Sanders AR, Zheng Y, Pe'er I, Dudbridge F, Holmans PA,
670   Whittemore AS, Mowry BJ, Olincy A, Amin F, Cloninger CR, Silverman JM, Buccola NG, Byerley
671   WF, Black DW, Crowe RR, Oksenberg JR, Mirel DB, Kendler KS, Freedman R, Gejman PV:
672   Common variants on chromosome 6p22.1 are associated with schizophrenia. Nature
673   2009;460:753-757.
674   43   Muller FJ, Schuldt BM, Williams R, Mason D, Altun G, Papapetrou EP, Danner S,
675   Goldmann JE, Herbst A, Schmidt NO, Aldenhoff JB, Laurent LC, Loring JF: A bioinformatic assay
676   for pluripotency in human cells. Nat Methods 2011;8:315-317.
677   44   Weissbein U, Schachter M, Egli D, Benvenisty N: Analysis of chromosomal aberrations
678   and recombination by allelic bias in RNA-Seq. Nat Commun 2016;7:12144.
679   45   Buskin A, Zhu L, Chichagova V, Basu B, Mozaffari-Jovin S, Dolan D, Droop A, Collin J,
680   Bronstein R, Mehrotra S, Farkas M, Hilgen G, White K, Pan KT, Treumann A, Hallam D, Bialas K,
681   Chung G, Mellough C, Ding Y, Krasnogor N, Przyborski S, Zwolinski S, Al-Aama J, Alharthi S, Xu Y,
682   Wheway G, Szymanska K, McKibbin M, Inglehearn CF, Elliott DJ, Lindsay S, Ali RR, Steel DH,
683   Armstrong L, Sernagor E, Urlaub H, Pierce E, Luhrmann R, Grellscheid SN, Johnson CA, Lako M:
684   Disrupted alternative splicing for genes implicated in splicing and ciliogenesis causes PRPF31
685   retinitis pigmentosa. Nat Commun 2018;9:4234.
686   46   Hadjicharalambous MR, Roux BT, Feghali-Bostwick CA, Murray LA, Clarke DL, Lindsay
687   MA: Long Non-coding RNAs Are Central Regulators of the IL-1beta-Induced Inflammatory
688   Response in Normal and Idiopathic Pulmonary Lung Fibroblasts. Front Immunol 2018;9:2906.
689   47   Bolger AM, Lohse M, Usadel B: Trimmomatic: a flexible trimmer for Illumina sequence
690   data. Bioinformatics 2014;30:2114-2120.
691   48   Dobin A, Davis CA, Schlesinger F, Drenkow J, Zaleski C, Jha S, Batut P, Chaisson M,
692   Gingeras TR: STAR: ultrafast universal RNA-seq aligner. Bioinformatics 2013;29:15-21.
693   49   Liao Y, Smyth GK, Shi W: featureCounts: an efficient general purpose program for
694   assigning sequence reads to genomic features. Bioinformatics 2014;30:923-930.
695   50   Durinck S, Spellman PT, Birney E, Huber W: Mapping identifiers for the integration of
696   genomic datasets with the R/Bioconductor package biomaRt. Nat Protoc 2009;4:1184-1191.
697   51   Hansen KD, Irizarry RA, Wu Z: Removing technical variability in RNA-seq data using
698   conditional quantile normalization. Biostatistics 2012;13:204-216.
699   52   Robinson MD, McCarthy DJ, Smyth GK: edgeR: a Bioconductor package for differential
700   expression analysis of digital gene expression data. Bioinformatics 2010;26:139-140.
701   53   Witten DM: Classification and clustering of sequencing data using a Poisson model. Ann
702   Appl Stat 2011;5:2493-2518.
703   54   Skene NG, Grant SG: Identification of Vulnerable Cell Types in Major Brain Disorders
704   Using Single Cell Transcriptomes and Expression Weighted Cell Type Enrichment. Frontiers in
705   neuroscience 2016;10:16.
706   55   Nalls MA, Consortium IPsDG: Expanding Parkinson's disease genetics: novel risk loci,
707   genomic context, causal insights and heritable risk. BioRxiv 2019
708   56   Consortium. SWGotPG: Biological insights from 108 schizophrenia-associated genetic
709   loci. Nature 2014;511:421-427.
710   57   Wray NR, Ripke S, Mattheisen M, Trzaskowski M, Byrne EM, Abdellaoui A, Adams MJ,
711   Agerbo E, Air TM, Andlauer TMF, Bacanu SA, Baekvad-Hansen M, Beekman AFT, Bigdeli TB,
712   Binder EB, Blackwood DRH, Bryois J, Buttenschon HN, Bybjerg-Grauholm J, Cai N, Castelao E,

713   Christensen JH, Clarke TK, Coleman JIR, Colodro-Conde L, Couvy-Duchesne B, Craddock N,
714   Crawford GE, Crowley CA, Dashti HS, Davies G, Deary IJ, Degenhardt F, Derks EM, Direk N, Dolan
715   CV, Dunn EC, Eley TC, Eriksson N, Escott-Price V, Kiadeh FHF, Finucane HK, Forstner AJ, Frank J,
716   Gaspar HA, Gill M, Giusti-Rodriguez P, Goes FS, Gordon SD, Grove J, Hall LS, Hannon E, Hansen
717   CS, Hansen TF, Herms S, Hickie IB, Hoffmann P, Homuth G, Horn C, Hottenga JJ, Hougaard DM,
718   Hu M, Hyde CL, Ising M, Jansen R, Jin F, Jorgenson E, Knowles JA, Kohane IS, Kraft J, Kretzschmar
719   WW, Krogh J, Kutalik Z, Lane JM, Li Y, Li Y, Lind PA, Liu X, Lu L, MacIntyre DJ, MacKinnon DF,
720   Maier RM, Maier W, Marchini J, Mbarek H, McGrath P, McGuffin P, Medland SE, Mehta D,
721   Middeldorp CM, Mihailov E, Milaneschi Y, Milani L, Mill J, Mondimore FM, Montgomery GW,
722   Mostafavi S, Mullins N, Nauck M, Ng B, Nivard MG, Nyholt DR, O'Reilly PF, Oskarsson H, Owen
723   MJ, Painter JN, Pedersen CB, Pedersen MG, Peterson RE, Pettersson E, Peyrot WJ, Pistis G,
724   Posthuma D, Purcell SM, Quiroz JA, Qvist P, Rice JP, Riley BP, Rivera M, Saeed Mirza S, Saxena R,
725   Schoevers R, Schulte EC, Shen L, Shi J, Shyn SI, Sigurdsson E, Sinnamon GBC, Smit JH, Smith DJ,
726   Stefansson H, Steinberg S, Stockmeier CA, Streit F, Strohmaier J, Tansey KE, Teismann H,
727   Teumer A, Thompson W, Thomson PA, Thorgeirsson TE, Tian C, Traylor M, Treutlein J,
728   Trubetskoy V, Uitterlinden AG, Umbricht D, Van der Auwera S, van Hemert AM, Viktorin A,
729   Visscher PM, Wang Y, Webb BT, Weinsheimer SM, Wellmann J, Willemsen G, Witt SH, Wu Y, Xi
730   HS, Yang J, Zhang F, eQtlgen, andMe, Arolt V, Baune BT, Berger K, Boomsma DI, Cichon S,
731   Dannlowski U, de Geus ECJ, DePaulo JR, Domenici E, Domschke K, Esko T, Grabe HJ, Hamilton
732   SP, Hayward C, Heath AC, Hinds DA, Kendler KS, Kloiber S, Lewis G, Li QS, Lucae S, Madden PFA,
733   Magnusson PK, Martin NG, McIntosh AM, Metspalu A, Mors O, Mortensen PB, Muller-Myhsok
734   B, Nordentoft M, Nothen MM, O'Donovan MC, Paciga SA, Pedersen NL, Penninx B, Perlis RH,
735   Porteous DJ, Potash JB, Preisig M, Rietschel M, Schaefer C, Schulze TG, Smoller JW, Stefansson
736   K, Tiemeier H, Uher R, Volzke H, Weissman MM, Werge T, Winslow AR, Lewis CM, Levinson DF,
737   Breen G, Borglum AD, Sullivan PF, Major Depressive Disorder Working Group of the Psychiatric
738   Genomics C: Genome-wide association analyses identify 44 risk variants and refine the genetic
739   architecture of major depression. Nat Genet 2018;50:668-681.
740   58   Stahl EA, Breen G, Forstner AJ, McQuillin A, Ripke S, Trubetskoy V, Mattheisen M, Wang
741   Y, Coleman JRI, Gaspar HA, de Leeuw CA, Steinberg S, Whitehead Pavlides JM, Trzaskowski M,
742   Pers TH, Holmans PA, Abbott L, Agerbo E, Akil H, Albani D, Alliey-Rodriguez N, Als TD, Anjorin A,
743   Antilla V, Awasthi S, Badner JA, Bækvad-Hansen M, Barchas JD, Bass N, Bauer M, Belliveau R,
744   Bergen SE, Bøcker Pedersen C, Bøen E, Boks M, Boocock J, Budde M, Bunney W, Burmeister M,
745   Bybjerg-Grauholm J, Byerley W, Casas M, Cerrato F, Cervantes P, Chambert K, Charney AW,
746   Chen D, Churchhouse C, Clarke T-K, Coryell W, Craig DW, Cruceanu C, Curtis D, Czerski PM, Dale
747   AM, de Jong S, Degenhardt F, Del-Favero J, DePaulo JR, Djurovic S, Dobbyn AL, Dumont A,
748   Elvsåshagen T, Escott-Price V, Fan CC, Fischer SB, Flickinger M, Foroud TM, Forty L, Frank J,
749   Fraser C, Freimer NB, Frisén L, Gade K, Gage D, Garnham J, Giambartolomei C, Giørtz Pedersen
750   M, Goldstein J, Gordon SD, Gordon-Smith K, Green EK, Green MJ, Greenwood TA, Grove J, Guan
751   W, Parra J, Hamshere ML, Hautzinger M, Heilbronner U, Herms S, Hipolito M, Hoffmann P,
752   Holland D, Huckins L, Jamain S, Johnson JS, Juréus A, Kandaswamy R, Karlsson R, Kennedy JL,
753   Kittel-Schneider S, Knott SV, Knowles JA, Kogevinas M, Koller AC, Kupka R, Lavebratt C,
754   Lawrence J, Lawson WB, Leber M, Lee PH, Levy SE, Li JZ, Liu C, Lucae S, Maaser A, MacIntyre DJ,
755   Mahon PB, Maier W, Martinsson L, McCarroll S, McGuffin P, McInnis MG, McKay JD, Medeiros
756   H, Medland SE, Meng F, Milani L, Montgomery GW, Morris DW, Mühleisen TW, Mullins N,

757 Nguyen H, Nievergelt CM, Adolfsson AN, Nwulia EA, O'Donovan C, Olde Loohuis LM, Ori APS,
758 Oruc L, Ösby U, Perlis RH, Perry A, Pfennig A, Potash JB, Purcell SM, Regeer EJ, Reif A, Reinbold
759 CS, Rice JP, Rivas F, Rivera M, Roussos P, Ruderfer DM, Ryu E, Sánchez-Mora C, Schatzberg AF,
760 Scheftner WA, Schork NJ, Weickert CS, Shehktman T, Shilling PD, Sigurdsson E, Slaney C,
761 Smeland OB, Sobell JL, Søholm Hansen C, Spijker AT, St Clair D, Steffens M, Strauss JS, Streit F,
762 Strohmaier J, Szelinger S, Thompson RC, Thorgeirsson TE, Treutlein J, Vedder H, Wang W,
763 Watson SJ, Weickert TW, Witt SH, Xi S, Xu W, Young AH, Zandi P, Zhang P, Zollner S, Adolfsson
764 R, Agartz I, Alda M, Backlund L, Baune BT, Bellivier F, Berrettini WH, Biernacka JM, Blackwood
765 DHR, Boehnke M, Børglum AD, Corvin A, Craddock N, Daly MJ, Dannlowski U, Esko T, Etain B,
766 Frye M, Fullerton JM, Gershon ES, Gill M, Goes F, Grigoroiu-Serbanescu M, Hauser J, Hougaard
767 DM, Hultman CM, Jones I, Jones LA, Kahn R, Kirov G, Landén M, Leboyer M, Lewis CM, Li QS,
768 Lissowska J, Martin NG, Mayoral F, McElroy SL, McIntosh AM, McMahon FJ, Melle I, Metspalu
769 A, Mitchell PB, Morken G, Mors O, Mortensen PB, Müller-Myhsok B, Myers RM, Neale BM,
770 Nimgaonkar V, Nordentoft M, Nöthen MM, O'Donovan MC, Oedegaard KJ, Owen MJ, Paciga SA,
771 Pato C, Pato MT, Posthuma D, Ramos-Quiroga JA, Ribasés M, Rietschel M, Rouleau GA, Schalling
772 M, Schofield PR, Schulze TG, Serretti A, Smoller JW, Stefansson H, Stefansson K, Stordal E,
773 Sullivan PF, Turecki G, Vaaler AE, Vieta E, Vincent JB, Werge T, Nurnberger JI, Wray NR, Di Florio
774 A, Edenberg HJ, Cichon S, Ophoff RA, Scott LJ, Andreassen OA, Kelsoe J, Sklar P: Genome-wide
775 association study identifies 30 Loci Associated with Bipolar Disorder. bioRxiv 2018:173062.
776 59   Grove J, Ripke S, Als TD, Mattheisen M, Walters RK, Won H, Pallesen J, Agerbo E,
777 Andreassen OA, Anney R, Awashti S, Belliveau R, Bettella F, Buxbaum JD, Bybjerg-Grauholm J,
778 Baekvad-Hansen M, Cerrato F, Chambert K, Christensen JH, Churchhouse C, Dellenvall K,
779 Demontis D, De Rubeis S, Devlin B, Djurovic S, Dumont AL, Goldstein JI, Hansen CS, Hauberg ME,
780 Hollegaard MV, Hope S, Howrigan DP, Huang H, Hultman CM, Klei L, Maller J, Martin J, Martin
781 AR, Moran JL, Nyegaard M, Naerland T, Palmer DS, Palotie A, Pedersen CB, Pedersen MG,
782 dPoterba T, Poulsen JB, Pourcain BS, Qvist P, Rehnstrom K, Reichenberg A, Reichert J, Robinson
783 EB, Roeder K, Roussos P, Saemundsen E, Sandin S, Satterstrom FK, Davey Smith G, Stefansson H,
784 Steinberg S, Stevens CR, Sullivan PF, Turley P, Walters GB, Xu X, Autism Spectrum Disorder
785 Working Group of the Psychiatric Genomics C, Bupgen, Major Depressive Disorder Working
786 Group of the Psychiatric Genomics C, andMe Research T, Stefansson K, Geschwind DH,
787 Nordentoft M, Hougaard DM, Werge T, Mors O, Mortensen PB, Neale BM, Daly MJ, Borglum
788 AD: Identification of common genetic risk variants for autism spectrum disorder. Nat Genet
789 2019;51:431-444.
790 60   Yengo L, Sidorenko J, Kemper KE, Zheng Z, Wood AR, Weedon MN, Frayling TM,
791 Hirschhorn J, Yang J, Visscher PM, Consortium G: Meta-analysis of genome-wide association
792 studies for height and body mass index in approximately 700000 individuals of European
793 ancestry. Hum Mol Genet 2018;27:3641-3649.
794 61   Genomes Project C, Auton A, Brooks LD, Durbin RM, Garrison EP, Kang HM, Korbel JO,
795 Marchini JL, McCarthy S, McVean GA, Abecasis GR: A global reference for human genetic
796 variation. Nature 2015;526:68-74.
797

798 **Acknowledgements**

802   **Author contribution**

803   A.K. performed the experiments, analyzed the data, and wrote the manuscript. R.B. analyzed

804   data, performed bioinformatic analysis and wrote the manuscript. S.Z. performed the initial

805   analysis of the RNA-seq data. H.Z. and M.S. performed the lab experiments. A.R.S, K.L., Z.P.P

806   and P.V.G helped interpret the results and edited the manuscript. J.D. conceived the study,

807   supervised the experiments and analyses, and wrote the manuscript.

808

809   **Competing Interests**

810   The authors have no competing interests to declare.

811

812   **Figure Legends**

813   **Figure 1. Generation of hi-PSC derived microglia (iMG).** (a) hiPSC lines iPS11 and iPS21

814   are differentiated to microglia lines CD11 and CD21, respectively, via embryoid bodies (EB) and

815   primitive macrophage precursors (PMP) over a period of 24 days. PMPs are produced

816   continuously in culture and are terminally differentiated into microglia when required. CD21 and

817   CD11 samples with a delta (Δ) denote iPMP samples and a dagger (†) denotes mixed samples

818   containing non-iMG cells. (b) DIC images of EB at day 6 (far left), iMG cells at day 24 (near left,

819   CD11-5) and more mature microglia cells at day 44 (far right, CD11-5). Some of the iMG

820   cultures also had non-iMG cells (near right, CD21-3), which morphologically resembled

821   fibroblasts. Scale bars at 500 μm. (c) Immunofluorescence staining of iMG from line CD11 at

822   day 24 shows expression of microglial/macrophage markers TREM2, CD45, and PU1. Scale

823   bars in 20x images are 100 μm, scale bars in 60x images are 50 μm. (d) The majority of the

824   iMG cells from line CD11 show expression of microglial/macrophage markers TREM2, CD45

825   and PU1, n=4-5. (e) Expression by qPCR of AD risk genes (BIN1, CLU, CD2AP, APOE,

826   TREM2) in different cell types (normalized to GAPDH). iAstro – hi-PSC derived astrocytes; iN-

827   Glut – hi-PSC derived glutaminergic neurons; NPC – neural progenitor cells.

828

829   **Figure 2. hi-PSC derived microglia (iMG) phagocytic activity is similar to primary**

830   **microglia.** Fluorescence imaging of day 27 iMG showing (a-c) time-dependent phagocytosis of

831   pHrodo labeled *E. coli*, colored red after ingestion. (d) This process is inhibited by the addition of

832   cytochalasin D. Percentages are of pHrodo-positive cell counts. All scale bars 100 μm, bright-

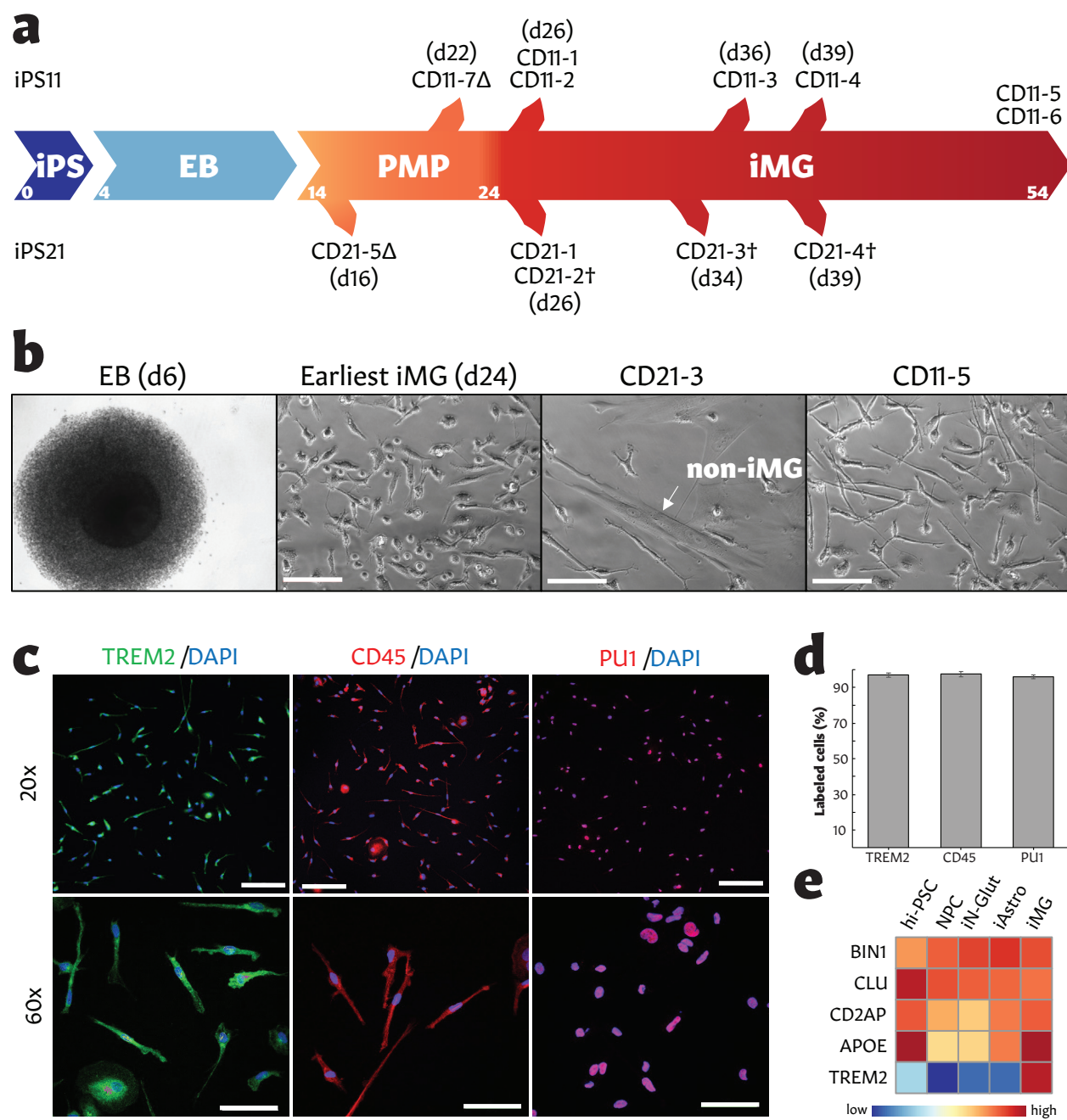833   field unavailable at 30 min.

834

835   **Figure 3. Transcriptional profiling of hi-PSC derived microglia (iMG).** (a) The first two

836   principal components of various human cellular lineages compared to induced microglia and

837   primitive macrophage precursors. Transcriptomic profiles are assessed on 15,469 quantile

838   normalized genes which are differentially expressed across all groups. Samples generated in

839   this study are denoted with an asterisk and grey outlines. DC – dendritic cells; Fib – fibroblasts

840   (lung and retinal tissue derived); iHPC – induced hematopoietic progenitor cells; iMG – induced

841   microglia (squares denote samples from Brownjohn et al., circles denote samples from Abud et

842   al.); iPMP - induced primitive macrophage precursors; iPS - induced pluripotent stem cells; MC

843   – monocytes; MGL – primary microglia (adult and fetal); Mixed – contaminated iMG cell lines;

844   NPC - neural progenitor cells. (b) Pairwise Poisson distance between raw protein-coding gene

845   counts. CD21 and CD11 samples are those generated in this study, with a delta (Δ) denoting

846   iPMP samples and a dagger (†) denoting mixed samples. AB – Abud et al. iMG samples; aMGL

847   – adult microglia; BJ – Brownjohn et al. iMG/iPMP samples; fMGL – fetal microglia; lFib – lung

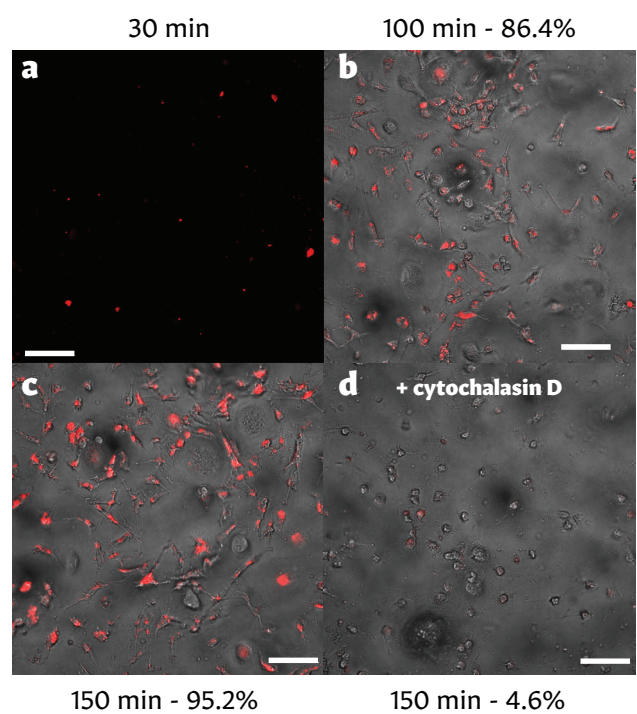848   tissue derived fibroblast; rFib – retinal tissue derived fibroblast.

849

Figure 4. Genetic relevance of hi-PSC derived microglia (iMG) to Alzheimer's Disease

(AD). (a) Quantile normalized RNA expression in 31 genes associated with AD risk (Haenseler

et al., 2017). Columns are individual samples annotated above by cell type. CD21 and CD11

samples are those generated in this study, with a delta (∆) denoting induced primitive

macrophage precursor (iPMP) samples and a dagger (†) denoting Mixed samples

(contaminated iMG cell lines). AB – Abud et al. iMG samples; aMGL – adult microglia; BJ –

Brownjohn et al. iMG/iPMP samples; DC – dendritic cells; Fib – fibroblasts (lung and retina

derived); fMGL – fetal microglia; iHPC – induced hematopoietic progenitor cells; iPS – induced

pluripotent stem cells; lFib – lung tissue derived fibroblast; MC – monocytes; MGL – primary

microglia (adult and fetal); NPC – neural progenitor cells; rFib – retinal tissue derived fibroblast.

(b) Distributions of gene specificities for each cell type, colored by decile. Single-cell RNA-Seq

cell types from Darmanis et al. (2015) are highlighted in navy. Ast – astrocytes; Endo – neural

endothelial cells; Neu – neurons; Olig – oligodendrocytes; scMGL – single-cell microglia. (c) AD

GWAS loci (Jansen et al., 2019) enrichment for LDSC and MAGMA across cell types, with a

Bonferroni threshold at α = 0.05 / (9 cell types x 7 GWAS traits). (d) A heatmap of LDSC (left)

and MAGMA (right) GWAS enrichment significance for AD, Schizophrenia (SCZ; PGC SCZ2,

2014), Parkinson's disease (PD; Nalls et al., 2019), major depressive disorder (MDD; Wray et

al., 2018), bipolar disorder (BIP; Stahl et al., 2018), autism spectrum disorder (ASD; Grove et

al., 2019), and body mass index (BMI; Yengo et al., 2018) across multiple cell types.

Enrichments with Bonferroni adjusted significance shown with bold borders.

a

iPS11

(d22)
CD11-7Δ

(d26)
CD11-1
CD11-2

(d36)
CD11-3

(d39)
CD11-4

CD11-5
CD11-6

iPS | EB | PMP | iMG
0 | 4 | 14 | 24 | 54

iPS21

CD21-5Δ
(d16)

CD21-1
CD21-2†
(d26)

CD21-3†
(d34)

CD21-4†
(d39)

b

EB (d6) | Earliest iMG (d24) | CD21-3 | CD11-5

non-iMG

c

TREM2 /DAPI | CD45 /DAPI | PU1 /DAPI

20x

60x

d

Labeled cells (%)

TREM2 | CD45 | PU1

e

hi-PSC | NPC | iN-Glut | iAstro | iMG

BIN1
CLU
CD2AP
APOE
TREM2

low — high

Figure 1

30 min   100 min - 86.4%

a

b

c

d   + cytochalasin D

150 min - 95.2%   150 min - 4.6%

Figure 2

Figure 3